Applied Acoustics 82 (2014) 45–52

Contents lists available at ScienceDirect

Applied Acoustics

journal homepage: www.elsevier.com/locate/apacoust

Prediction model of flow duct constriction noise

Oscar Kårekull [a,b,*], Gunilla Efraimsson [c], Mats Åbom [a]

[a] Marcus Wallenberg Laboratory, KTH, Stockholm, Sweden
[b] Fläkt Woods, 551 84 Jönköping, Sweden
[c] Aeronautical and Vehicle Engineering, KTH, Stockholm, Sweden

ARTICLE INFO

Article history:
Received 16 October 2013
Received in revised form 11 February 2014
Accepted 3 March 2014
Available online 29 March 2014

Keywords:
Flow noise
Noise prediction
RANS

ABSTRACT

The scaling law for aerodynamic dipole type of sound from constrictions in low speed flow ducts by Nelson and Morfey is revisited. A summary of earlier published results using this scaling law is presented together with some new data. Based on this, an effort to find a general scaling law for the sound power for components with both distinct and non-distinct flow separation points are made. Special care is taken to apply the same scaling to all data based on the pressure drop. Results from both rectangular and circular ducts, duct flow velocities from 2 to 120 m/s and sound power measurements made both in ducts and in reverberation chambers are presented. The computed sound power represents the downstream source output in a reflection free duct. In particular for the low frequency plane wave range strong reflections from e.g. openings can affect the sound power output. This is handled by reformulating the Nelson and Morfey model in the form of an active acoustic 2-port. The pressure loss information needed for the semi-empirical scaling law can be gained from CFD simulations. A method using Reynold Average Navier Stokes (RANS) simulations is presented, where the required mesh quality is evaluated and estimation of the dipole source strength via the use of the pressure drop is compared to using the turbulent kinetic energy.

1. Introduction

Accurate determination of flow generated noise from constrictions in low speed ducts can be done by measurements. Assuming broad-band sound generation with no distinct harmonics in the spectrum, i.e., excluding non-linear aeroacoustic phenomena such as whistling, the measurements can be done using standard methods for sound power [1]. In low Mach number confined flows separation at a constriction corresponds to a compact dipole source due to an unsteady force acting on the fluid. An alternative to experiments is to simulate the broad band sound generation using Computational Fluid Dynamics (CFD). However such system require a complex simulation, e.g. full compressible Large Eddy Simulation (LES), and is still a significant challenge not useful for everyday engineering practice. The need is often to predict an approximate level of the flow noise for a particular case, avoiding spending the time to make the measurement or conduct the full simulation analysis.

As shown by Nelson and Morfey [1], using a generalized spectrum, the flow noise generation in low speed flow ducts can, if the effect of incoming turbulence is neglected by assuming a homogeneous inflow, be approximated from the component pressure drop. The pressure drop or the equivalent pressure loss coefficient can be obtained from standard measurements or possibly from relatively fast CFD models such as Reynold Average Navier Stokes (RANS) simulations.

A reduction of energy consumption in todays society is in great focus and the pressure drop is closely related to energy losses in the system. Since it is already used in the product development process, e.g. for ventilation products, the use of pressure drop is suitable as an model input. By determining a set of spectra for different constriction geometries, having either a distinct point of flow separation e.g. orifices, or a non-distinct, e.g. dampers or bends, a generalized model for noise prediction would be available. This paper intends to review previously published measurement data applying the same scaling to all the data in order to see common trends in the dimensionless noise spectra. Furthermore, the possibility to use a CFD approach to estimate the dipole strength of a duct component is addressed.

Iudin initiated the concept of noise prediction from air duct elements creating flow separation in 1955 [2], but Nelson and Morfey

* Corresponding author at: Fläkt Woods, 551 84 Jönköping, Sweden. Tel.: +46 36193546.
E-mail address: oscar.karekull@flaktwoods.com (O. Kårekull).

http://dx.doi.org/10.1016/j.apacoust.2014.03.001
0003-682X/

are normally cited as having created the foundation for the more recent work on the subject by their publication from 1981 [1]. They were inspired by the work on flow spoilers by Gordon [3,4]. But also by the work on the correlation between the noise radiation and the fluctuating forces on flow spoilers by Heller and Widnall [5]. The Nelson and Morfey model was derived using dipole characteristics of the noise sources together with the assumption that the rms fluctuating drag force acting on the component is proportional to the steady state drag force. In Ref. [1] the steady state drag force was determined by measurements of the component pressure drop and the duct area. The model was verified via measurements in a rectangular flow duct connected to a reverberation chamber. Test objects were a number of strip spoilers and some orifice type geometries created as inverted strip spoilers in rectangular ducts. As detailed below over the years a number of papers based on Nelson and Morfeys scaling model have been published.

Oldham and Ukpoho [6] continued the work determining the component open area ratio and characteristics dimensions (vena contracta) from the measured pressure drop. This new definition enables components with more complex geometries to be scaled. Oldham et al. also extended the model to include circular ducts. Measurements were conducted on circular dampers at different angles and circular orifices with different diameters. Waddington and Oldham [7] measured the spectra for mitred bends in rectangular ducts and Oldham and Waddington [8] investigated the similarity when altering the air velocity and duct dimensions of different types of bends.

Gijrath et al. [9] analyzed a number of bends by estimating the generated sound power from measurements of the sound pressure level in a duct. Effects of rounding inner and outer corners of the bends were also investigate together with an analysis of the Mach number dependency. Nygård [10] introduced the concept of 2-ports, to handle wave interaction effects in the plane wave range, and compared the simulation results from a 2-port simulation code to measurement results. Different bend geometries were analyzed and also the interaction of two bends with a defined in-between distance was measured. Two bends were concluded as independent sources if the in-between distance was at least 8 duct diameters. An in-duct measurement setup similar to the one by Gijrath et al. [9] was used.

Allam and Åbom [11] continued the use of 2-ports and investigated an orifice geometry by induct measurements comparing the up and downstream side. Both passive, scattering properties, as well as active, noise generating, properties were determined in the plane wave range using a method proposed by Lavrentjev et al. [12]. It can be noted that the data in Ref. [11] unlike all other reported data gives a complete aeroacoustic description of the orifice. The data is measured so that in principle all boundary effects are eliminated, thereby representing the correct up- and downstream sound power in an infinite duct. The interaction of two orifices at a varied in-between distance was also investigated and the sources were concluded independent at an in-between distance of at least 7 duct diameters. Ducret [13] investigated the sound generation for bends in tailpipe applications. Noise generation and scaling laws for different bend radius were analyzed. Measurements in a reverberation chamber were conducted using ducts with 1–5 diameters of duct length after the bends. Tailpipe diffusers were analyzed using different diffuser angles.

Mak et al. [14] measured strip spoilers with similar geometries to the ones in [1] but for lower Strouhal numbers. A second and a third strip spoiler were introduced and the flow noise was predicted by determining the drag forces and their phase relationship together with the coherence function of the noise sources. In a series of papers Mak et al. [15–17] also investigated the possibility to gain the dipole force information from CFD simulations. In the model developed, the averaged turbulent kinetic energy was used instead of the pressure drop directly as dipole input data. Reynolds Average Navier Stokes (RANS) simulations gave the averaged turbulent kinetic energy in each node of the calculation mesh and a relationship between the drag force and the total turbulent kinetic energy in selected nodes was used in combination with a reference spectrum to create the dipole input data. Also in a recent work Mak et al. [18] has applied Large-Eddy Simulations (LES) to estimate the fluctuating dipole.

Besides the work following [1], general guidelines and reference spectra for air conditioning systems can be found in e.g. ASHREA Handbook for HVAC Applications [19] or VDI 2081 Noise generation and noise reduction in air-conditioning systems [20]. These provide references to publications of measurement data for noise generation in e.g. ducts [21] and by duct elements [22]. Ingard et al. [22] did e.g. measurements on a rectangular damper at different angles a case which will be included in the review below.

The paper is divided into three sections. The first part defines the generalized description of the model including source and radiation characteristics together with system interaction properties in the plane wave region. The second part reviews measurement data for orifice, bend and damper geometries using the described model intending a reference spectrum generalization. Finally the third part compares two CFD approaches using RANS simulations analyzing mesh and turbulence model dependency.

2. Model for generalized predictions of flow noise

In this section a model based on the dipole forces of the flow noise source in combination with an acoustic radiation resistance for an infinite duct is described. Essentially the model is the same as the originally presented by Nelson and Morfey [1] but written in a form which better highlights the physical concepts involved. The original model [1] represents a power based approach not suited for the low frequency plane wave range. For the plane wave range the model for in duct constrictions is better expressed in the form of 2-ports [10] as presented in Section 2.3.

2.1. Source model

There are two main assumptions for the source model of Nelson and Morfey [1]. First low Mach numbers and a compact source or point is assumed. Secondly only dipole sound sources related to the flow separation and unsteady forces produced along the duct axis are included. This implies the sound pressure up or downstream of the flow separation to be the product of a force, F, and a function describing the radiation properties. The sound power in a frequency band, e.g., 1/3 octave, generated in one direction of the duct can then, in the frequency domain, be described by

$$W_D = R(He)|S_{FF}(St)|^2 \tag{1}$$

where S_{FF} is the force autospectrum as a function of a Strouhal number (St) and R is the radiation resistance for an infinite duct as a function of the duct Helmholtz number (He). Assuming that the force autospectrum can be split into a mean force $\overline{F}$ part and a source strength spectrum part K^2, the sound power can, when constants are included into R, be written as

$$W_D = R(He)\overline{F}^2K^2(St) \tag{2}$$

Note that the mean force is frequency independent. In [1], the mean force is defined for flow separation at a certain known point or cross section. This force can be related to the pressure drop over the element and the duct area A, as

$$\overline{F} = A \cdot \Delta P \tag{3}$$

where ΔP is the static pressure drop of the constriction. To generalize the concept to include other types of duct components, e.g. bends, dampers, not only elements with distinct flow separation points needs to be considered. In the following the pressure loss coefficient, C_L ,

$$C_L = \frac{\Delta P}{0.5\rho_0 U^2}. \tag{4}$$

will be used. C_L can be determined in different ways but can be found for the most common geometries in handbooks by e.g. Idelchick [23] or Blevins [24]. From measurements or simulations we can determine C_L from the pressure drop, ΔP, the mean flow velocity, U, and the air density, ρ_0 in the duct. It will also be used here to define the frequency scaling properties in the Strouhal number as it can be determined for all duct components independently of the flow separation properties.

Using Eqs. (2)–(4) the reference spectrum, K, as a function of the Strouhal number, can be formulated as

$$10log_{10}\left(K^2(St)\right) = Lw_D - 10log_{10}\left[R(He)C_L^2U^4\right] \tag{5}$$

where Lw_D is the generated sound power in the duct, U is the mean flow velocity in the duct, C_L is the pressure loss coefficient and W_{ref} for Lw_D is 10^{-12} W. The reference spectrum is defined as a function of the Strouhal number, St, which is chosen as

$$St = \frac{f_c d_c}{U_c} \tag{6}$$

where d_c is a characteristic dimension, U_c the component flow velocity and f_c is the band center frequency under consideration. It is to be observed that the exact choice of the ingoing length and velocity scales in the Strouhal number will influence the scaling of the reference spectrum. Oldham and Ukpoho [6] chose to define the open area ratio as a function of the pressure drop for an orifice. Assuming that this holds for other types of geometries this enables a generalization of the area ratio since a pressure loss coefficient can always be determined. The open area ratio can, from the pressure loss coefficient, be defined [6] as

$$\sigma = \frac{\sqrt{C_L} - 1}{C_L - 1}. \tag{7}$$

The geometry independent definition of the component openness can now be used to define the Strouhal number used. The mean air velocity in the component U_c can be defined as

$$U_c = \frac{U}{\sigma}. \tag{8}$$

The characteristic dimension can be determined, as the hydraulic diameter, by

$$d_c = \sqrt{\frac{4A\sigma}{\pi}}. \tag{9}$$

This yields a definition of the Strouhal number as

$$St = \frac{f_c\sigma\sqrt{\frac{4A\sigma}{\pi}}}{U}. \tag{10}$$

This general definition of the Strouhal number, using the pressure loss coefficient, enable the determination of open area ratios for complex geometries. It also avoids the dimension selection in a geometry where the dominating noise generating mechanism is not straight forward. However, it must be stressed that the main weakness of the proposed Strouhal scaling is related to the validity of Eq. (7) for an arbitrary flow case.

2.2. Source radiation dependence on duct cross section

The noise source caused by the duct constriction will interact with the modes of the duct cross section. The cut-on wave number k_0 is dependent on the duct cross area geometry. The first mode in a circular duct is defined by

$$k_0 = \frac{1.84}{r} \tag{11}$$

where r is the radius of the duct. The other common duct geometry is the rectangular duct and the cut-on is defined by

$$k_0 = \pi/max(2a, 2b) \tag{12}$$

where a and b are the dimensions of the duct. For the plane wave region, both in circular and rectangular ducts, the radiation resistance R is only dependent on the duct area. Above cut on all propagating modes needs to be considered and a summation of them will return the generated sound power as a function of the Helmholz number i.e. the wave number and duct dimension. The mode density will increase with increasing frequency and the prediction of a radiation resistance from a frequency averaged level will consequently become more accurate with increasing frequency. The average radiation resistance, rewritten from [1] for rectangular ducts and from Oldham and Waddington [6] for circular ducts, is given by

$$R_{pl.w.} = \frac{\rho_0 A}{8c_0} \qquad k < k_0 \tag{13}$$

$$R_{circ.d.} = \frac{\rho_0 A^2 k^2 (1 + (3\pi/4rk))}{48\pi c_0} \qquad k > k_0 \tag{14}$$

$$R_{rect.d.} = \frac{\rho_0 A^2 k^2 (1 + (3\pi/4k)(a+b)/A)}{48\pi c_0} \qquad k > k_0 \tag{15}$$

where A is the duct area, ρ_0 is the density of air and c_0 is the speed of sound in air. Compared to the plane wave region the last two formulas introduce a factor that for high frequencies converges to

$$\frac{k^2 A}{6\pi} \tag{16}$$

which is equivalent to a component radiating as a dipole in free field.

A fundamental assumption of the model [1] is that the dipole source is not blocking the duct i.e. acts as a point source at an arbitrary point in a duct cross-section. If the characteristic dimension of the duct constriction is much smaller than the duct diameter, the basic assumption might not be applicable any more. As an example consider an orifice plate where the orifice diameter is much smaller than the duct diameter. For this limit it seems more appropriate to model the sound generation as a fluctuating force acting on the hole impedance producing an oscillating volume flow.

2.3. Sound source interaction with duct system

The sound power from the semi-empirical scaling laws represents the source output in a reflection free environment. In particular for the low frequency plane wave range strong reflections from e.g. duct openings has a non-negligible effect and wave based rather than power based models should be used. A sound source in a duct system can in the plane wave range then be modeled by introducing a 2-port, which for an acoustically compact sound source, i.e. for a quasi-steady and incompressible flow, is derived by e.g. Gijrath et al. [25]. The result for the passive (scattering) part is

$$\begin{pmatrix} p_{1-} \\ p_{2-} \end{pmatrix} = S\begin{pmatrix} p_{1+} \\ p_{2+} \end{pmatrix} = \frac{1}{2 + MC_L}\begin{bmatrix} MC_L & 2 \\ 2 & MC_L \end{bmatrix}\begin{pmatrix} p_{1+} \\ p_{2+} \end{pmatrix} \tag{17}$$

where the subscripts 1 and 2 denote the up- and downstream side, +/− waves propagating into or out from the system, $M = U/c$ is the Mach number and S is the scattering matrix. From this model the transmission and reflection can, in the plane wave range of the constriction, be described only by the Mach number and the pressure loss coefficient. These would also be the input data for the noise predictions by the semi-empirical scaling laws.

The active part of the 2-port can be determined by the flow separation of the component which generates the upstream and downstream travelling pressure waves [25]. Introduced into the equation of the passive part the full 2-port model is given by [12]

$$\begin{pmatrix} p_{1-} \\ p_{2-} \end{pmatrix} = S \begin{pmatrix} p_{1+} \\ p_{2+} \end{pmatrix} + \begin{pmatrix} p^s_{1-} \\ p^s_{2-} \end{pmatrix} \tag{18}$$

The noise prediction from the semi-empirical scaling laws can then be implemented in the 2-port model as p^s given by

$$|p^s_{1-}|^2 = |p^s_{2-}|^2 = \frac{W_D \rho_0 c_0}{A} \tag{19}$$

$$p^s_{1-} = -p^s_{2-}. \tag{20}$$

The amplitude distribution is computed using the scaling law for the appropriate component, assuming a white noise distribution in each band [10]. The assumption of equal amplitudes in the up- and downstream directions can as shown by the measurement of Allam and Åbom [11] be questioned. However, since Ref. [11] is the only work that has reported this so far this effect is neglected here noting that more measurements including both up- and downstream is of interest.

The flow constriction properties for both noise generation, transmission and reflection can now be described using a model whose input is limited to the pressure loss coefficient and a reference spectrum. A possible generalization of the model would be to characterize the spectra ($K^2(St)$ see Eq. (5)) for different geometries and to gain the pressure loss coefficient, C_L, from CFD simulations. This can be seen as the main idea behind the present paper.

3. Generality of the semi-empirical scaling law

To evaluate the generality of the semi-empirical scaling law in Eq. (5) and especially the comparison between components with distinct and non-distinct flow separation points, different geometries need to be presented using the same scaling law model. Previously published measurement data corresponding to orifice, damper and bend geometries are here reanalyzed according to the scaling model presented in the previous chapter. The published cases can be grouped into the main cases with distinct or non-distinct flow separation points. Third octave band levels are used or a corresponding third octave band level when the original data is presented in octave bands. To recalculate a factor of 10log (1/3) has been subtracted from the octave band level assuming an equal level in each band.

Fig. 1 presents an overview of the component geometries studied: orifices, dampers and bends. Bends of 90° made by joining two pipes cut at 45° angle are called miter bends in both circular and rectangular ducts. When a number of sizes and/or flow velocities for a geometry have been measured an average of the measurements is presented. It can also be noted that all papers except Ref. [11] only studied the sound power emitted on the downstream side.

3.1. Orifices – distinct flow separation point

Four publications are used to review orifices. Measurement results by Nelson and Morfey [1] are for rectangular, sharp edged, orifices with thickness 3 mm, height 0.3 m and 0.1 m, 0.15 m and 0.2 m width, all placed in a 0.3 * 0.3 m rectangular duct. The duct was connected to a reverberation chamber where the sound power was measured. Nelson and Morfey reported an error in their presented data of 6 dB [6] and a correction for this has been introduced. Flow velocities between 2.5 and 27 m/s were used.

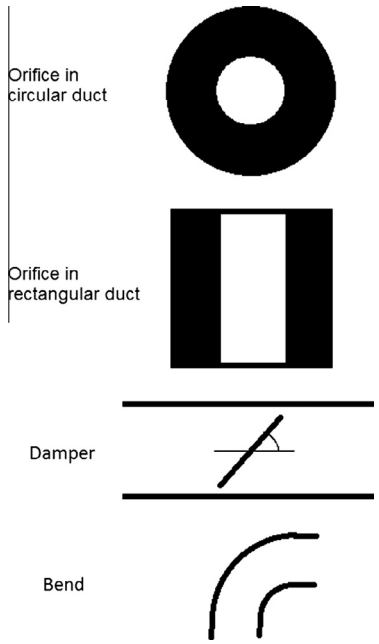

Fig. 1. Geometries studied. For dampers the opening angle must be specified. For smooth bends the radius of curvature is needed. Note that miter bends can have both rectangular and circular cross-section.

Oldham and Ukpoho [6] results corresponds to circular orifices with a diameter of 0.191 m, 0.216 m or 0.241 m, all in 0.300 m circular duct. Sound power was measured in a reverberation chamber and flow velocities between 8 and 18 m/s were used. Allam and Åbom [11] measured an orifice of diameter 0.03 m in a circular duct of 0.057 m. Sound generation was determined only in the plane wave range using a 2-port model and the flow velocities were varied between 15 and 34 m/s. Mak et al. [14] measured rectangular orifices corresponding to a height of 0.1 m and width of 0.025 m or 0.05 m, both placed in a 0.1 * 0.1 m rectangular duct connected to a reverberation chamber used for sound power determination. Flow velocities between 10 and 35 m/s were used. The Mach-number and He-number range for all publications are summarized in Table 1.

The data of the four publications are presented in Fig. 2. The results collapse well for Strouhal numbers larger than 1. The reference spectra for circular orifices have a trend of getting a change in inclination at or below Strouhal number equal to 1. This trend is not present in all the results for rectangular orifices. One explanation is that the data for rectangular orifices by Nelson and Morfey [1] are not measured for small enough St-numbers so a possible shift in inclination might not be visible. For the circular case there is a large difference between the data of Oldham and Ukpoho, and Allam and Åbom for St smaller than 1. From a measurement method perspective low frequencies introduce higher uncertainty (3 dB) when using the reverberation chamber method [26]. Here it is probable that the data of Allam and Åbom is better, since it is based on a method for extracting the in-duct plane wave sound power removing all reflections [10,12], see Section 2.3. In Fig. 2 an effort to construct a general orifice source strength spectrum has been made. The construction is based on, like also the cases for dampers and bends, the fact that all the data, for high frequencies, will fol-

Table 1
Flow velocities for the orifices.

Author	Flow velocity U (m/s)	He number range	Orifice shape
Nelson and Morfey [1]	2.5–27	0.08–3	Rectangular
Oldham and Ukpoho [6]	8–18	0.03–4	Circular
Allam and Åbom [11]	15–34	0.03–0.3	Circular
Mak et al. [14]	10–35	0.03–2	Rectangular

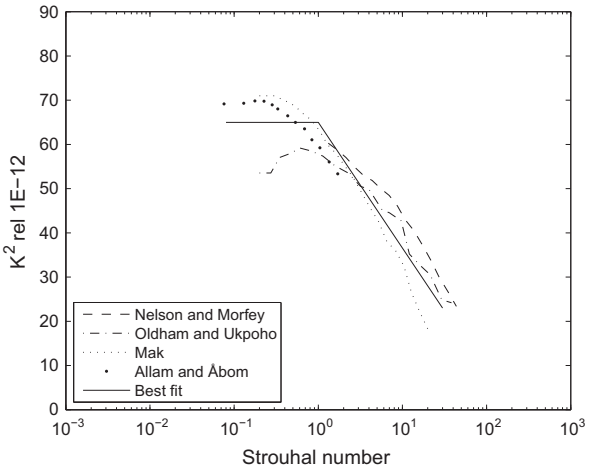

Fig. 2. Dimensionless source strength spectra for orifices.

low a slope of $-28\log(St)$, see Section 3.3. The curve can be described by

$$K^2(St) = 65 \quad St < 1 \tag{21}$$

$$K^2(St) = 65 - 28log(St) \quad St > 1 \tag{22}$$

3.2. Dampers and Bends – non-distinct flow separation point

From a geometrical perspective, orifices are of a two dimensional nature and has distinct flow separation while bends and dampers are of a three dimensional nature i.e. has non-distinct flow separation points.

Data for dampers from two publications are presented in Table 2. Measurement results by Oldham and Ukpoho [6] correspond to circular dampers at an angle 20°, 25° or 30° . The diameter of the damper was 0.3 m. The circular duct had an equivalent diameter. Sound power was measured in a reverberation chamber and flow velocities between 10 and 25 m/s were used.

Ingard et al. [22] measured a damper in a rectangular duct where both width and height were 0.61 m. The damper geometry had equivalent width and height and a thickness of 3 mm. Two damper angles of 15° and 45° were used and sound power was measured in a reverberation chamber. Flow velocities at 11 and 13 m/s were presented, but published results are described by Ingard et al. as typical for the velocity range 4–32 m/s.

Table 2
Flow velocities for the dampers.

Author	Flow velocity U (m/s)
Oldham and Ukpoho [6]	10–25
Ingard et al. [22]	11–13 (4–32)

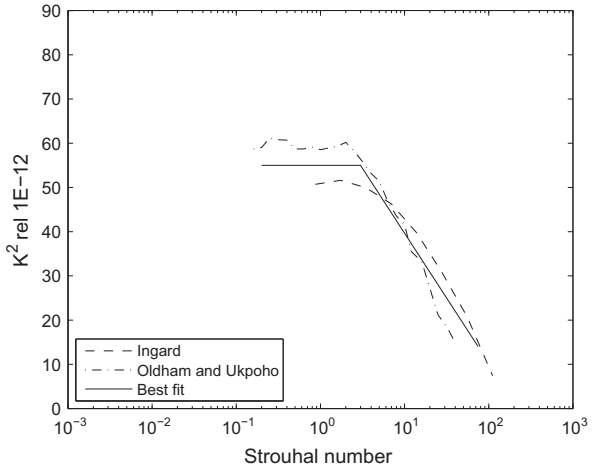

Fig. 3. Dimensionless source strength spectra for dampers.

Fig. 3 presents a comparison of the two publications where the results correlates well for higher Strouhal numbers. There is a trend of getting a change in inclination somewhere at low Strouhal numbers for both the Oldham and Ingard results. The shift seems to be at a higher Strouhal number than for the orifices. Again an effort to construct a general damper source strength spectrum has been made, see Fig. 3, the curve can be described by

$$K^2(St) = 55 \quad St < 3 \tag{23}$$

$$K^2(St) = 68 - 28log(St) \quad St > 3 \tag{24}$$

Data for bends originate from three publications and are summarized in Table 3. Measurement results by Waddington and Oldham [7] corresponds to miter bends in a rectangular duct with height and width of 0.6 m or 0.4 m. Sound power was measured in a reverberation chamber and duct flow velocities between 7 and 22 m/s were used.

Measurement results by Gijrath et al. [9] and Nygård [10] corresponds to a miter bend and a bend, denoted normal, having a radius of half the duct diameter, $r/D = 0.5$, in circular ducts of diameter 0.043 m. Sound power was measured using an in-duct microphone array. The data from Gijrath and Nygård are very similar and obtained from the same measurement setup. Flow velocities between 34 and 120 m/s were used.

Measurement results by Ducret [13] corresponds to both a 45° bend and a 90° bend. Results are available for both angles for dimension $r/D = 2.5$ but only to a 90° bend for dimension $r/D = 1.6$. The duct diameter was always 0.042 m. Sound power was measured in a reverberation chamber. Flow velocities between 23 and 80 m/s were used. The results are presented as one average of all duct diameters and flow velocities. Due to the nature of the exhaust tail pipe application of interest for the Ducret investigation, a length of only five duct diameters was used after the bend.

The data of the three publications presented in Fig. 4 collapse well. As for the other geometries a trend for a change in inclination at low Strouhal numbers appear. For bends this change is at or lower

Table 3
Flow velocities for bends.

Author	Flow velocity U (m/s)	Bend type
Waddington and Oldham [7]	7–22	Miter
Gijrath et al. [9]	34–120	Miter and $r/D = 0.5(90°)$
Ducret [13]	23–80	$r/D = 2.5(90°; 45°)$ and $1.6(90°)$

than Strouhal 1 for all three publications. A general bend source strength spectrum is presented in Fig. 4, it can be described by

$$K^2(St) = 77 \quad St < 0.5 \tag{25}$$

$$K^2(St) = 69 - 28log(St) \quad St > 0.5 \tag{26}$$

3.3. All components

An interesting question is to what extent a universal trend exist in the dimensionless source strength spectra for all components. Fig. 5 presents a comparison of the measurement data for orifices, bends and dampers. The spread is smaller for high Strouhal numbers than for low Strouhal numbers. The data collapses for geometries with both distinct and non-distinct flow separation for $St > 3$ demonstrating a weak dependence on the detailed geometry. For this range a first order polynomial least square best fit results in

$$K^2(St) = 68 - 28log(St) \quad St > 3 \tag{27}$$

All spectra approach a constant level at low Strouhal numbers but the level and St number where this occurs are strongly dependent on the geometrical details. For applications related to human hearing, e.g. by A-weighting, low frequencies can be considered as of less importance for the total level. Consequently deviations at low frequencies are not as critical when the total A-weighted level is of interest. It can be noted that in the high Strouhal number limit

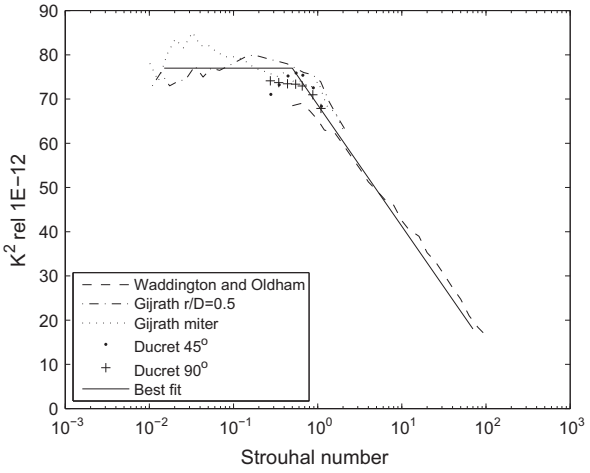

Fig. 4. Dimensionless source spectra for bends.

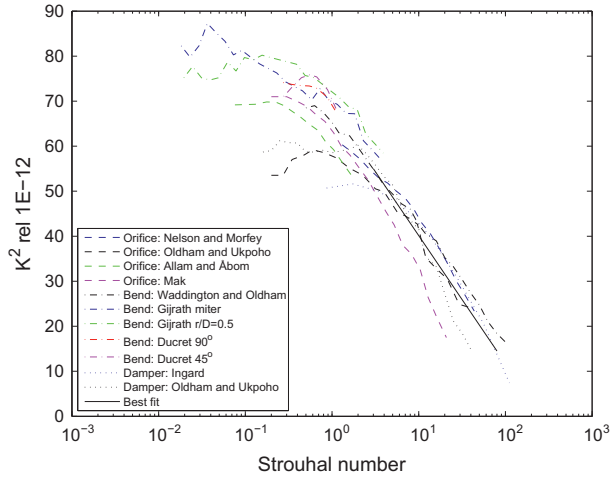

Fig. 5. Dimensionless source strength spectra for all components.

the trend for a pure (3D) dipole is $-20\log(St)$ and a pure (3D) quadropole $-40\log(St)$. Thus the found universal trend $-28\log(St)$ appears to be a mix of these source mechanisms. Finally as a comment on the accuracy of the proposed general scaling laws, Eqs. (21)–(26), the standard deviation in each band can be estimated to 2–3 dB.

4. Semi-empirical scaling laws based on CFD data

In the previous section, the reference spectrum of the semi-empirical scaling law was studied. In this section, the term in Eq. (2) related to the pressure loss is considered and the possibility to use Computational Fluid Dynamics (CFD) data in the determination of the pressure drop is evaluated.

In industrial applications, noise predictions using CFD often aim at predicting an approximate level of the flow noise without spending the time to make either measurements or conduct a high resolution simulation analysis. Using semi-empirical scaling laws, the flow noise generation in low speed flow ducts can be approximated from the mean force of the flow acting on a constriction [1]. The mean force can be determined using either measurements or possibly the use of CFD simulations e.g. Reynold Average Navier Stokes (RANS) simulations. Two different models to predict the sound power through the use of RANS simulations and a noise reference spectrum are compared and evaluated by Karekull and Efraimsson in Ref. [27]. One model predicts the sound power based on the pressure drop whereas the other model uses the turbulent kinetic energy [17]. For completeness we here include some results, illustrating the strengths and weaknesses of the two models.

In order to numerically simulate the air flow, some part of the turbulent field needs to be modeled. In RANS simulations, the whole turbulent part of the flow is modeled, yielding averaged flow quantities without detailed turbulence information. This approach is less costly than e.g. Large-Eddy Simulations (LES), where part of the turbulent field is resolved in the simulations whereas the smaller scales, and their influence of the larger structures, are modeled.

From a RANS simulation, the input data needed for the semi-empirical scaling laws is available. For the first approach, the static pressure drop over the duct constriction is needed. The pressure drop is readily obtained from a RANS simulation.

An other way to use RANS data is proposed by Mak and Au [17] and is based on the turbulent kinetic energy. The turbulent velocity field is related to the turbulent kinetic energy, k, given by

$$k = \frac{1}{2}\sum u_j^2 \tag{28}$$

where u_j is the turbulent velocity in j the three space dimensions. In a RANS simulation, k is determined by the equation for the turbulent kinetic energy within the turbulence model obtained for each cell in the computational domain. For a chosen area the summation of k in the corresponding cells enable an equivalent measure to the fluctuating velocity and the mean force, related to the pressure drop across a constriction, can be determined from the turbulent kinetic energy by

$$\overline{F} = C\rho_0 \sum A_i k_i. \tag{29}$$

Here A_i is the corresponding surface at the constriction from which the turbulent kinetic energy k_i is determined. For simplicity, the model constant C can, as presented by Mak and Au [17], be included into the spectrum part K. Together with the reference spectrum, a compensation for the duct area size and the air properties, the generated sound power is calculated by

$$Lw_D = 10log_{10}\left(K^2\right) + 10log_{10}\left[\frac{\rho_0}{4Ac_0}\right] - 20log_{10}\left[\sum A_i k_i\right] \tag{30}$$

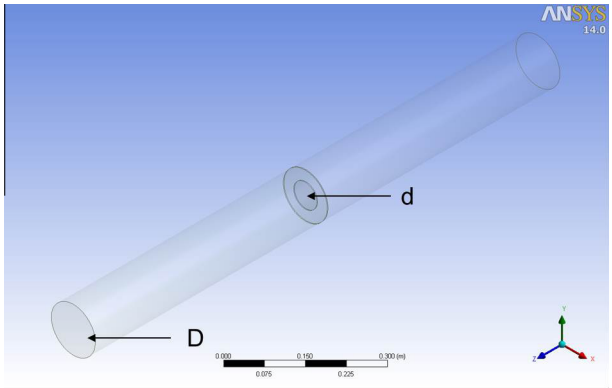

Fig. 6. Orifice in circular duct.

Table 4
Dimensions of orifice in circular duct.

Duct diameter D (m)	0.057
Duct length upstream of orifice	20D
Duct length downstream of orifice	10D
Orifice diameter d (m)	0.03
Orifice thickness (m)	0.002

The flow through an orifice in a cylindrical pipe has been considered for the evaluation of the two approaches. The orifice is positioned in the middle of a circular duct which extends both upstream and downstream as presented in Fig. 6 with the corresponding dimensions presented in Table 4. Noise data for the orifice is available from Allam and Åbom [11] for the duct flow velocities 15, 23 and 34 m/s.

RANS simulations were conducted using the commercial CFD software package Ansys CFX 14. The meshes were generated by ICEM CFD Tetra mesher. The incompressible Reynolds Average Navier Stokes equations were solved in double precision using a second order finite volume scheme for the discretisation in space. In the simulations, the inlet boundary condition was set to a mean flow velocity (15, 23, 34 m/s). The turbulence level at the inflow boundary was set to 10% with a turbulence dimension of the duct diameter. The outlet boundary condition was set to 101,325 Pa static pressure as a mean over the duct outlet area. At the solid walls, no slip wall boundary conditions were used.

Two mesh structures were evaluated, one fine semi-structured mesh using hexagonal mesh elements with both a shear layer and boundary layer grid and a more industrial like mesh, easily generated by a commercial software, using triangular elements and only the boundary layer specially resolved. The meshes are presented in Fig. 7 and consisted both of approximately $2 * 10^6$ nodes.

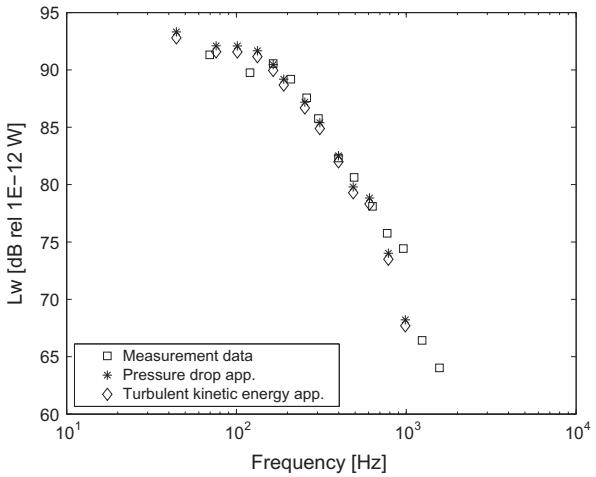

Fig. 8. Evaluation of pressure drop and turbulent kinetic energy noise prediction approaches at 15 m/s.

Three turbulence models were studied, namely k–ω SST [28], BSL [29] and BSL EARSM [30]. For a two equation eddy viscosity turbulence model a common opinion, e.g. [31], is that the k–ω SST has a satisfying performance. A further step in model complexity would be to use Reynold stress models. Two versions of Reynolds stress models have been tested: BSL and BSL EARSM. Both models could bring more accuracy to the results. Using the standard mesh the accuracy of the noise prediction did not increase using neither BSL EARSM nor BSL Reynold stress compared to using k–ω-SST. In addition the simulations had problems to converge for the semi structured mesh with the use of the more complex turbulence models. Using more advanced turbulence models or meshes was not seen to improve the accuracy in order to motivate the increased computational complexity.

Simulations with changed duct lengths upstream of the orifice showed that decreasing the duct length upstream of the orifice below 20D increased the error. Increasing the length to 30D did however only improve the accuracy negligibly.

Fig. 8 presents a comparison of the resulting sound power from the two approaches. The accuracy of both approaches is satisfying. The area for summation of the k calculation is not strictly defined in [17]. The selection of in-data positions will depend on the constriction geometry and the flow separation. Hence, a more detailed knowledge of the noise generation mechanisms for the constriction is needed when using the turbulent kinetic energy approach. In addition the reference spectrum, K, will be similar to the reference spectrum in the pressure drop model but not identical depending on the model constant, C, and the choice of the corresponding surface for the calculation of k. An alternative is to use

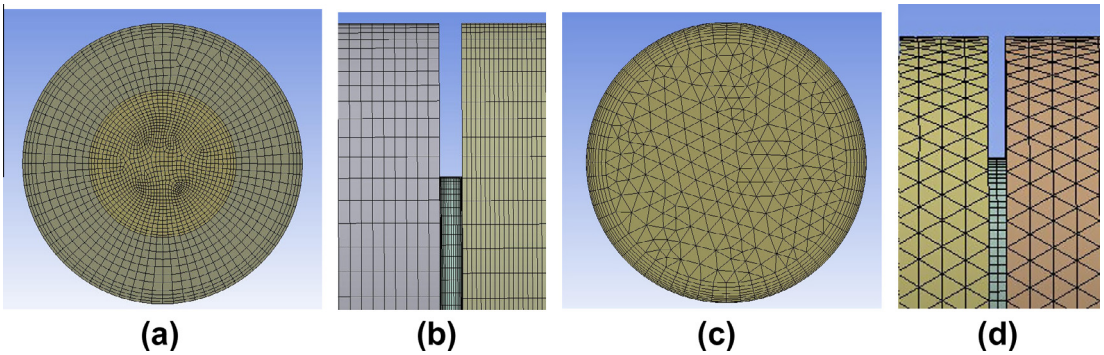

Fig. 7. Semi structured ((a) and (b)) and standard mesh ((c) and (d)).

RANS data to compute the pressure drop directly. It eliminates the uncertainty of guessing the correct domain for the estimation of turbulent kinetic energy and replace this with a standard result i.e. the pressure drop. This type of result can typically be estimated with an accuracy better than 10% using standard mesh solutions.

5. Conclusions

The noise prediction method proposed by Nelson and Morfey [1] is revisited and a Strouhal-number scaling based on pressure drop or pressure loss coefficient is proposed. This scaling makes it easier to apply the method to more complex constrictions. This has been demonstrated by applying this approach to find general scaling laws for orifices, dampers and bends, see Eqs. (21)–(26). Plotting all the constrictions together the dimensionless source spectra also show a "universal" collapse for high Strouhal-numbers, see Fig. 5. In addition the possibility to obtain the pressure drop required for the noise prediction model via RANS data is addressed. It is found that this can work well even using a standard mesh and turbulence models. More details of that study is found in Ref. [27]. Finally the need to reformulate the Nelson and Morfey model for the low frequency plane wave range is pointed out. For this range the model can be reformulated in terms of acoustic 2-ports, thereby enabling modeling of wave interaction effects which can be important at low frequencies [10].

This analysis and all publications referred to are assuming a homogeneous inflow to the constriction. Noise predictions for turbulent inflow to constrictions at low Mach number flows are planned as future work.

Acknowledgments

The work reported in this paper is supported by the Swedish Research Council Formas, project 245-2011-1615, and by Fläkt Woods.

References

[1] Nelson PA, Morfey CL. Aerodynamic sound prediction in low speed flow ducts. J Sound Vib 1981;79:263–89.
[2] Iudin EI. The acoustic power of the noise created by airduct elements. Sov Phys Acoust 1955;1:383–98.
[3] Gordon CG. Spoiler-generated flow noise. I: The experiments. J Acoust Soc Am 1968;43:1041–8.
[4] Gordon CG. Spoiler-generated flow noise. II: Results. J Acoust Soc Am 1969;45:214–23.
[5] Heller HH, Widnall SE. Sound radiation from rigid flow spoilers correlated with fluctuating forces. J Acoust Soc Am 1970;47:924–36.
[6] Oldham DJ, Ukpoho AU. A pressure-based technique for predicting regenerated noise levels in ventilation systems. J Sound Vib 1990;140:259–72.
[7] Waddington DC, Oldham DJ. Generalized flow noise prediction curves for air duct elements. J Sound Vib 1999;222:163–9.
[8] Oldham DJ, Waddington DC. The prediction of airflow-generated noise in ducts from considerations of similarity. J Sound Vib 2001;248(4):780–7.
[9] Gijrath JWM, Verhaar BT, Bruggeman JC. Prediction model for broadband noise in bends. Delft, TNO Institute of Applied Physics; 1999.
[10] Nygård S. Modeling of low frequency sound in duct networks. Licentiate Thesis. Department of Aeronautical and Vehicle engineering, Royal Institute of Technology, Stockholm, Sweden; 2000
[11] Allam S, Åbom M. Aero-acoustic study of single and double diaphragm orifices under subsonic conditions. Royal Institute of Technology, Stockholm, Sweden; 2005
[12] Lavrentjev J, Åbom M, Bodén H. A measurement method for determining the source data of acoustic two-port sources. J Sound Vib 1995;183(3):517–31.
[13] Ducret F. Studies of sound generation and propagation in ducts. Licentiate Thesis. Department of Aeronautical and Vehicle engineering, Royal Institute of Technology, Stockholm, Sweden; 2006.
[14] Mak CM, Wu J, Ye C, Yang J. Flow noise from spoilers in ducts. J Acoust Soc Am 2009;125(6):3756–65.
[15] Mak CM, Oldham DJ. The application of computational fluid dynamics to the prediction of flow generated noise in low speed ducts: Part 1: Fluctuating drag forces on a flow spoiler. J Build Acoust 1997;5(2):123–41.
[16] Mak CM, Oldham DJ. The application of computational fluid dynamics to the prediction of flow generated noise: Part 2: Turbulence-based prediction technique. J Build Acoust 1998;5(3):199–213.
[17] Mak CM, Au WM. A turbulence-based prediction technique for flow-generated noise produced by in-duct elements in a ventilation system. Appl Acoust 2009;70:11–20.
[18] Mak CM, Wang X, Ai ZT. Prediction of flow noise from in-duct spoilers using computational fluid dynamics. Appl Acoust 2014;76:386–90.
[19] ASHRAE Handbook – HVAC Applications (SI). ISBN 9781936504084. Section 47.7–47.10; 2007.
[20] VDI 2081 Part 1. Noise generation and noise reduction in air-conditioning systems. ICS 17.140.20; 2001. p. 26–36.
[21] Bullock CE. Aerodynamic sound generation by duct elements. ASHREA Trans 1970;76(2):97–109.
[22] Ingard U, Oppenheim A, Hirshorn M. Noise generation in ducts. A SHREA Trans 1968;74(1):V1.1–V1.10.
[23] Idelchik IE. Handbook of hydraulic resistance. 2nd ed.. Berlin: Springer Verlag; 1986.
[24] Blevins RD. Applied fluid dynamics handbook. New York: Van Nostrand Reinhold; 1984.
[25] Gijrath H, Nygård S, Åbom M. Modelling of flow generated sound in ducts. In: The 8th international conference of sound and vibration; 2001.
[26] ISO 3741 acoustics – determination of sound power levels and sound energy levels of noise sources using sound pressure – precision methods for reverberation test rooms.
[27] Kårekull O, Efraimsson G. Comparison of RANS parameters for flow noise prediction. Internoise 2013, Paper 0403; 2013.
[28] Menter FR. Improved two-equation k–w turbulence models for aerodynamic flows. NASA Tech. Memo. 103975, NASA Ames CA; 1992.
[29] Menter FR. Multiscale model for turbulent flows. In: 24th Fluid dynamics conference. American Institute of Aeronautics and Astronautics; 1993.
[30] Wallin S, Johansson A. A complete explicit algebraic Reynolds stress model for incompressible and compressible flows. J Fluid Mech 2000;403:89–132.
[31] Casey M, Wintergerste T. ERCOFTAC Best Practice Guidelines Quality and Trust in Industrial CFD Version 1.0; 2000.